

LA-UR-17-21923 (Accepted Manuscript)

Ultra-thin metasurface microwave flat lens for broadband applications

Azad, Abul Kalam Efimov, Anatoly V. Ghosh, Shuprio Singleton, John Taylor, Antoinette Jane Chen, Houtong

Provided by the author(s) and the Los Alamos National Laboratory (2017-11-12).

To be published in: Applied Physics Letters

DOI to publisher's version: 10.1063/1.4984219

Permalink to record: http://permalink.lanl.gov/object/view?what=info:lanl-repo/lareport/LA-UR-17-21923

Disclaimer:

Approved for public release. Los Alamos National Laboratory, an affirmative action/equal opportunity employer, is operated by the Los Alamos National Security, LLC for the National Nuclear Security Administration of the U.S. Department of Energy under contract DE-AC52-06NA25396. Los Alamos National Laboratory strongly supports academic freedom and a researcher's right to publish; as an institution, however, the Laboratory does not endorse the viewpoint of a publication or guarantee its technical correctness.



Ultra-thin metasurface microwave flat lens for broadband applications

Abul K. Azad¹*, Anatoly V. Efimov¹, Shuprio Ghosh¹, John Singleton², Antoinette J. Taylor³, and Hou-Tong Chen¹

¹Center for Integrated Nanotechnologies, Los Alamos National Laboratory, MS K771, Los Alamos,

New Mexico 87545, USA

² Condensed Matter and Magnet Science, Los Alamos National Laboratory, MS E536, Los Alamos,

New Mexico 87545, USA

³ Chemistry, Life and Earth Sciences, Los Alamos National Laboratory, MS F629, Los Alamos, New

Mexico 87545, USA

* Electronic address: aazad@lanl.gov

ABSTRACT: We demonstrate a metasurface-based ultrathin flat lens operating at microwave

frequencies. A series of subwavelength metallic split-ring resonators (SRRs), which are sandwiched

between two cross-polarized metallic gratings, are defined to obtain a radially symmetric parabolic

phase distribution, covering relative phase differences ranging from 0 to 2.5π radians, to create a lens.

The tri-layer lens demonstrates focusing/collimating of broadband microwave radiations from 7.0 to

10.0 GHz, with a gain enhancement of 17 dBi at the central wavelength 9.0 GHz while fed by a

rectangular horn antenna. The measured focal length agrees reasonably well with design, achieving a

3dB directionality < 4.5° and confirming high-quality beam collimation along the propagation direction.

The demonstrated metasurface flat lens enable light-weight, low-cost, and easily deployable flat

transceivers for microwave communication, detection, and imaging applications.

Long-haul microwave communications require components such as reflectors and lenses for collimating/focusing microwaves to efficiently transmit/receive information. Critical considerations for these components include high gain, broad operational bandwidth, light-weight, easy deployment, and low cost. Parabolic dish antennas have been the most commonly used beam collimating/focusing devices in microwave communication links. However, their output may interfere with the feed antenna [1] and cause feed blockage for a center-fed configuration, and is sensitive to the positioning of the feed antenna while using an offset-fed configuration. Dielectric lenses mitigate some of these limitations, but they are generally bulky and heavy, because they rely on the spatially dependent phase accumulation introduced by geometric shaping of lens materials with sufficient thickness and dielectric-constant contrast to that of air. The introduction of Fresnel zoned plate lenses reduces the thickness; however, they suffer from zone edge blockage and typically low efficiencies [1, 2]. Microwave lens antennas were also demonstrated using arrays of constrained patch antennas [3, 4], where the required phase retardations were obtained by controlling the lengths of microstrips that connect the patches from front side to back side of the lens. However, the operational bandwidths of these lens antennas were only a few percent due to the well-known narrowband nature of patch antennas. While the operational bandwidth could be improved by introducing multi-layer frequency selective surfaces with precise alignments between layers [5], the overall gain remained much inferior compared to that of a traditional dish antenna. Therefore, alternative techniques have been sought to enable light-weight, ultrathin, flat lenses for broadband operation with high efficiency, including metamaterial based gradient index lens [6, 7] and Luneburg lens [8, 9].

Metasurfaces, the two-dimensional equivalent of metamaterials, have shown unprecedented capability in manipulating electromagnetic waves [10-13], enabling unique electromagnetic phenomena such as anomalous refraction/reflection [14, 15], polarization conversion [16, 17], flat lensing [18, 19], broadband hologram [20, 21], electromagnetic phase-shifting [22], to name a few. Unlike bulk

ultrathin metasurfaces introduce electromagnetic media, abrupt phase discontinuities reflected/transmitted beams via resonances in subwavelength resonators, where the scattering amplitude and phase can be controlled through tuning their geometric parameters. Therefore, metasurfaces are capable of engineering wavefronts of the transmitted/reflected beams at will by introducing spatially variant amplitude/phase profiles through rationale design of subwavelength resonators, leading to ultrathin planar optical devices [23]. Recently, ultrathin plasmonic metasurface-based flat lenses have been demonstrated at optical [18, 19, 24] and terahertz [25, 26] frequencies, which enable planar integration of light-weight lenses in an optical system to overcome the limitations of conventional lenses. While these devices exhibit unprecedented capabilities in manipulating electromagnetic waves, their performances still suffer from low efficiency due to limited scattering efficiencies [10, 18]. There are a few attempts to enhance beam-focusing efficiency, but most of these metasurface devices work in reflection geometry [27, 28]. While dielectric metasurface lenses have demonstrated higher focusing efficiencies in transmission mode in the optical frequency range [29, 30], the requirements of high permittivity dielectric resonators, relatively large resonator size, and the correspondingly increasing weight pose significant challenge in fabrication and deployment.

Here, we demonstrate a metasurface flat lens based on a tri-layer metasurface concept adapted from our previous demonstration of high-efficiency broadband linear polarization converters [16]. It significantly improves the performance of microwave beam collimation/focus in transmission mode at frequencies centered on 9.0 GHz. The measurements reveal excellent collimation of the output beam with a gain enhancement of 17 dBi.

The schematic design of the tri-layer metasurface is shown in Fig. 1(a), consisting of a subwavelength, anisotropic, metallic resonator array sandwiched between a pair of orthogonally oriented subwavelength metal gratings. The first metal grating, which is arranged to be transparent for the incident waves with grating wires perpendicular to the polarization of the incident waves, allows for the incident waves

interaction with the anisotropic split-ring resonators (SRRs) which have symmetry axes along the diagonal directions. This interaction of incident waves with SRRs converts the incident waves into coand cross-polarized waves scattering in both forward and backward directions after transmitting through and reflecting from the resonator array. The cross-polarized forward-scattering waves can pass through the second metal grating as desired, while the co-polarized forward-propagating waves are blocked and reflected back to the resonator array, allowing for additional interaction and polarization conversion. On the other hand, the cross-polarized backward-scattering waves are blocked and reflected to the desirable forward-direction by the first grating, while the co-polarized backward-scattering waves pass through the first grating, causing reflection losses. The arrangement of the three layers of metasurfaces forms a Fabry-Pérot-like cavity, enabling multiple reflections and polarization conversions within the cavity, therefore significantly enhancing the overall polarization conversion efficiency [16]. By appropriately adjusting the spacing distance as well as the resonator geometric parameters, the overall co-polarized reflection can be minimized due to the destructive interference of the multiple reflections [31]. As a result, the tri-layer metasurface structure is able to rotate the polarization of the incident microwave by 90° with a very high efficiency over a broadband frequency range, as shown in Fig. 1(b). By varying the geometric parameters of the anisotropic SRRs, the phase of the cross-polarized transmission can be tuned to cover the entire range of 2.5 π at a specific operational frequency, which is required for constructing a metasurface flat lens. Figure 1(b) shows the numerically simulated transmission amplitude and phase spectra for two *uniform* tri-layer metasurfaces using different resonator structures.

The design of our metasurface lens has been guided by the conventional lens formula and the relative phase progression as a function of radius r from the center is

$$\Delta \varphi = \frac{2\pi}{\lambda} \left(\sqrt{f^2 + r^2} - f \right), \tag{1}$$

shown by the inset cyan solid curve in Fig. 2(a), where f is the designed focal length of the lens and λ is the operating wavelength. For simplicity, we divide the metasurface lens into 22 annular zones with the same width equal to the unit cell size of 10 mm. At each zone we digitize the phase value following the theoretical curve, therefore requiring 22 designs of resonators with corresponding phase values to construct our metasurface lens; and Figure 1(c) summarizes the transmission amplitude and phase at 9.0 GHz for the designed 22 different resonators. Although the resonators form a square array, the distribution of different resonator designs is based on their center positions falling to particular zones. The inset to Fig. 1(c) shows the schematic design of a SRR, where the geometric parameters are varied to form the 22 designs. By tuning the length L_1 , the gap size (through varying L_2), and the gap position of the SRR, we obtain the required scattering phase through carrying out full-wave numerical simulations using CST Microwave Studio for the tri-layer metasurface containing resonators in a uniform and infinite array. In doing this, we have assumed that the scattering phase from an individual resonator within the metasurface lens is the same as that of an infinite 2D resonator array. For our particular design of metasurface lens, the relative phase values of the 22 resonators are between 0 to 2.5π radians, as shown by the symbols in Fig. 1(c) for the operational frequency of 9 GHz. It is important to note here that in these simulations the transmission has also been maximized, which is shown also in Fig. 1(c), to achieve highest possible gain.

The front and back metal gratings consist of arrays of copper lines of width 1 mm and thickness 17 μ m, with a period of 2 mm. The gratings and the resonator array (with an area of $46 \times 46 \text{ mm}^2$) are fabricated on commercially available low loss dielectric substrates by chemical etching of the double copper cladding printed circuit boards (PCBs) from Rogers Corporation (RO 4003C, thickness 0.508 mm). The back-side copper cladding of each layer has been completely etched away. A dielectric constant of 3.55 and a loss tangent of 0.0027 have been used in all numerical simulations during the design. The three layers are separated from each other by an air-gap of 5 mm and the total thickness of the metasurface

lens antenna is 11.5 mm. The fabricated SRR layer is shown in Fig. 2(a), with the 22 SRR elements shown in Fig. 2(a) bottom inset, distributed along the radial direction from center to the edge of the lens to enable the required phase distributions. All of these SRRs are defined by a fixed arm length $L_1 = 7.5$ mm, line width w = 1 mm, and a variable length of arm L_2 , except for SRR # 5, 6, 7, and 20 where $L_1 = 7.2$ mm, 8.0 mm, 8.0 mm, and 7.2 mm, respectively, in order to maintain a transmission higher than 90%.

The fabricated metasurface lens was characterized inside an anechoic chamber using a pair of broadband horn antennas (SAS-571) and a vector network analyzer (Agilent N5230A). The horn antennas were aligned carefully along the optical axis of the lens for the line of sight measurement as shown in Fig. 2(b). The lens was placed at a distance d_1 =53 cm (designed focal length) from the feed horn antenna (transmitter) while the distance between the detector and the lens (d_2) was 11 m (far field). As the design of our metasurface lens introduced 90° rotation of the linear polarization, we correspondingly rotated the detector by 90° relative to the feed horn antenna to measure the metasurface lens output.

Figure 3(a) depicts the measured angle-dependent gains of a horn antenna at 9.0 GHz with and without the metasurface lens. It is worth mentioning here that, when measuring the gain of the feed-horn antenna without the metasurface lens, the polarization of both horns was parallel to measure the co-polarized component. The results clearly show the gain enhancement as we compare the measurements with (blue curve) and without (black-curve) the metasurface lens. The horn-feed metasurface lens antenna shows a total gain of 29 dBi, which is approximately17 dB higher than the gain of the feed-horn alone (\approx 12 dBi), validating our design of metasurface lens for microwave beam collimation. The measured gain of the metasurface lens antenna show side lobes, with the first side lobe appearing at \pm 7° and 17 dB lower than the main lobe, whereas the gain of the feed-horn alone exhibits a slight monotonic decay within our measured angle range. These side lobes are introduced by diffraction from the edge of metasurface lens, as the incident beam from the rectangular horn antenna is larger than the metasurface lens. The side

lobes could be further reduced by increasing the size of the metasurface lens and optimizing the irradiation area using a polarization-maintaining circular horn antenna. The measured difference between the transmitted co- and cross-polarized components is 35 dB, indicating a pure linear polarization conversion as expected from our metasurface design scheme. We calculate the gain of an ideal parabolic reflecting dish antenna of the same size with a typical antenna efficiency (60%) [32], which gives \approx 30 dBi, comparable to the measured gain of \sim 29 dBi in our horn-feed metasurface lens antenna, and indicating the high efficiency of linear polarization conversion in the metasurface lens. The small difference in the gains may be attributed to the discretized phase progression in the metasurface lens introduced by the finite size of the SRRs compared to the continuous phase progression in the reflecting dish.

The directivity of an antenna is an important parameter for long-haul communications. The measured 3dB directionality of our antenna is less than 4.5°, indicating a good collimation of the radiative power along the boresight from the feed horn antenna. The measured directionality is comparable to typical dish antennas, which makes our metasurface lens antenna a promising candidate for point-to-point microwave communication. The small asymmetry in the measured gain curve may have been caused from the slight miss-alignment of the feed or detection horns with the lens optical axis. Another important criterion of a microwave communication link is the operational bandwidth that defines the data handling capability. The growing need for high speed data transmission demands further improvement of the operational bandwidth for space born communication. We measured the frequency-dependent gain enhancement of the metasurface lens at frequencies ranging from 3 GHz to 15 GHz. The measured 3-dB bandwidth is about 3 GHz, extending from 7 GHz to 10 GHz, which is higher than in previously demonstrated flat lenses [3-5].

To verify the beam collimation through our metasurface lens, we measured the far-field radiation pattern by scanning both azimuthal (horizontal or pan) and the tilting (vertical or tilt) angles of the horn-feed metasurface lens while keeping the receiver fixed. The measured 2D field distribution at 9 GHz is shown in Fig. 3(b). In good agreement with the 1D scanning, the radiation is characterized by a dominant Gaussian main lobe with 3-dB gain enhancement angle consistently less than 4.5°, followed by side lobes with the 1st side lobe consistently 17 dB lower. We observed a small deviation in the angular symmetry of the side lobes, which may arise from the slight missalignment between the lens and the horn antennas. Also, the non-uniform irradiation of the metasurface lens by the rectangular horn-feed antenna may partially contribute to the asymmetric power distribution in the higher-order lobes. A circular feed-horn antenna, carefully centered at the focal point of the metasurface lens, may improve the symmetry and increase the gain of the main lobe further.

Finally, by varying the distance (d_I) between the lens and the feed-horn antenna from 35 to 100 cm with an increment of 1 cm, we measured the power distributions in a plane containing the optical axis of the metasurface lens. For each d_I the pan (or azimuth) angle was scanned from -20° to 20°. The 2D plots are shown in Fig. 4 for the measured power at different frequencies as a function of distance d_I and pan angle. These measurement show equivalently the focusing capability of the metasurface lens at different frequencies. We notice a gradual shifting of the focal point to a longer distance as the frequency increases. The 3-dB power concentration distance along the optical axis at 9 GHz extends from d_I = 49 cm to 56 cm. The maximum power concentration was observed at d_I = 53 cm, which is reasonably close to the designed focal length (f = 50 cm) at 9.0 GHz. The small discrepancy may be attributed to the paraxial ray approximation in designing our metasurface lens. Despite of the frequency-dependent focal length, our measurements revealed 4 GHz operational bandwidth when placing the feed antenna at the focal position denoted by the black dotted lines in Fig. 4.

In conclusion, we have designed, fabricated, and characterized a highly efficient flat metasurface lens at microwave frequencies based on a tri-layer metasurface architecture consisting of an anisotropic resonator array sandwiched between a pair of orthogonal metal gratings. The fabricated metasurface lens

demonstrates excellent collimation of the radiated microwaves from a feed-horn antenna. The measured results show a gain enhancement as high as 17 dBi (60 times) in addition to the 12 dBi gain from the feed horn antenna. The ultra-thin flat metasurface lens, fabricated from commercially available PCB techniques, may be further applied to flexible substrates, and enable next generation light-weight, flat, and deployable microwave lens antennas for long-haul communication links.

This work was performed, in part, at the Center for Integrated Nanotechnologies, a U.S. Department of Energy, Office of Basic Energy Sciences Nanoscale Science Research Center operated jointly by Los Alamos and Sandia National Laboratories. Los Alamos National Laboratory, an affirmative action/equal opportunity employer, is operated by Los Alamos National Security, LLC, for the National Nuclear Security Administration of the U.S. Department of Energy under Contract No. DE-AC52-06NA25396. We acknowledge supports from the LDRD program, Los Alamos National Laboratory.

References:

- [1] W. Rotman, "Analysis of an EHF aplanatic zoned dielectric lens antenna," *IEEE Transactions on Antennas and Propagation* **32**, 611-617 (1984).
- [2] H. D. Hristov and M. H. A. J. Herben, "Millimeter-wave Fresnel-zone plate lens and antenna," *IEEE Transactions on Microwave Theory and Techniques* **43**, 2779-2785 (1995).
- [3] D. McGrath, "Planar three-dimensional constrained lenses," *IEEE Transactions on Antennas and Propagation* **34**, 46-50 (1986).
- [4] P. M. P. Daniel T. McGrath, Mark A. Mehalic, "The microstrip constrained lens," *Microwave Journal* **38**, 24 (1995).
- [5] M. Li, M. A. Al-Joumayly, and N. Behdad, "Broadband True-Time-Delay Microwave Lenses Based on Miniaturized Element Frequency Selective Surfaces," *IEEE Transactions on Antennas and Propagation* **61**, 1166-1179 (2013).
- [6] T. Driscoll, D. N. Basov, A. F. Starr, P. M. Rye, S. Nemat-Nasser, D. Schurig, and D. R. Smith, "Free-space microwave focusing by a negative-index gradient lens," *Applied Physics Letters* **88**, 081101 (2006).
- [7] R. B. Greegor, C. G. Parazzoli, J. A. Nielsen, M. A. Thompson, M. H. Tanielian, D. C. Vier, S. Schultz, D. R. Smith, and D. Schurig, "Microwave focusing and beam collimation using negative index of refraction lenses," *IET Microwaves, Antennas & Propagation* 1, 108-115 (2007).
- [8] N. Kundtz and D. R. Smith, "Extreme-angle broadband metamaterial lens," *Nat Mater* **9**, 129-132 (2010).
- [9] Q. Cheng, H. F. Ma, and T. J. Cui, "Broadband planar Luneburg lens based on complementary metamaterials," *Applied Physics Letters* **95**, 181901 (2009).
- [10] H.-T. Chen, A. J. Taylor, and N. Yu, "A review of metasurfaces: physics and applications," *Rep. Prog. Phys.* **79**, 076401 (2016).
- [11] S. B. Glybovski, S. A. Tretyakov, P. A. Belov, Y. S. Kivshar, and C. R. Simovski, "Metasurfaces: From microwaves to visible," *Physics Reports* **634**, 1-72 (2016).
- [12] N. F. Yu and F. Capasso, "Flat optics with designer metasurfaces," *Nat Mater* **13**, 139-150 (2014).
- [13] A. V. Kildishev, A. Boltasseva, and V. M. Shalaev, "Planar Photonics with Metasurfaces," *Science* **339**, (2013).
- [14] N. Yu, P. Genevet, M. A. Kats, F. Aieta, J.-P. Tetienne, F. Capasso, and Z. Gaburro, "Light Propagation with Phase Discontinuities: Generalized Laws of Reflection and Refraction," *Science* **334**, 333-337 (2011).
- [15] S. L. Sun, Q. He, S. Y. Xiao, Q. Xu, X. Li, and L. Zhou, "Gradient-index meta-surfaces as a bridge linking propagating waves and surface waves," *Nat Mater* **11**, 426-431 (2012).
- [16] N. K. Grady, J. E. Heyes, D. R. Chowdhury, Y. Zeng, M. T. Reiten, A. K. Azad, A. J. Taylor, D. A. R. Dalvit, and H.-T. Chen, "Terahertz Metamaterials for Linear Polarization Conversion and Anomalous Refraction," *Science* **340**, 1304-1307 (2013).
- [17] N. Yu, F. Aieta, P. Genevet, M. A. Kats, Z. Gaburro, and F. Capasso, "A Broadband, Background-Free Quarter-Wave Plate Based on Plasmonic Metasurfaces," *Nano Lett.* **12**, 6328-6333 (2012).
- [18] F. Aieta, P. Genevet, M. A. Kats, N. F. Yu, R. Blanchard, Z. Gahurro, and F. Capasso, "Aberration-free ultrathin flat lenses and axicons at telecom wavelengths based on plasmonic metasurfaces," *Nano Lett.* **12**, 4932-4936 (2012).

- [19] X. Ni, S. Ishii, A. V. Kildishev, and V. M. Shalaev, "Ultra-thin, planar, Babinet-inverted plasmonic metalenses," *Light Sci. Appl.* **2**, e72 (2013).
- [20] G. Zheng, H. Mühlenbernd, M. Kenney, G. Li, T. Zentgraf, and S. Zhang, "Metasurface holograms reaching 80% efficiency," *Nat Nano* **10**, 308-312 (2015).
- [21] Y. Yifat, M. Eitan, Z. Iluz, Y. Hanein, A. Boag, and J. Scheuer, "Highly Efficient and Broadband Wide-Angle Holography Using Patch-Dipole Nanoantenna Reflectarrays," *Nano Lett.* **14**, 2485-2490 (2014).
- [22] H.-T. Chen, W. J. Padilla, M. J. Cich, A. K. Azad, R. D. Averitt, and A. J. Taylor, "A metamaterial solid-state terahertz phase modulator," *Nat Photon* **3**, 148-151 (2009).
- [23] N. I. Zheludev and Y. S. Kivshar, "From metamaterials to metadevices," *Nat Mater* **11**, 917-924 (2012).
- [24] H.-S. Ee and R. Agarwal, "Tunable Metasurface and Flat Optical Zoom Lens on a Stretchable Substrate," *Nano Lett.* **16**, 2818-2823 (2016).
- [25] Q. Wang, X. Zhang, Y. Xu, Z. Tian, J. Gu, W. Yue, S. Zhang, J. Han, and W. Zhang, "A Broadband Metasurface-Based Terahertz Flat-Lens Array," *Adv. Opt. Mater.* **3**, 779-785 (2015).
- [26] X.-Y. Jiang, J.-S. Ye, J.-W. He, X.-K. Wang, D. Hu, S.-F. Feng, Q. Kan, and Y. Zhang, "An ultrathin terahertz lens with axial long focal depth based on metasurfaces," *Opt. Express* **21**, 30030-30038 (2013).
- [27] A. Pors, M. G. Nielsen, R. L. Eriksen, and S. I. Bozhevolnyi, "Broadband Focusing Flat Mirrors Based on Plasmonic Gradient Metasurfaces," *Nano Lett.* **13**, 829-834 (2013).
- [28] X. Li, S. Xiao, B. Cai, Q. He, T. J. Cui, and L. Zhou, "Flat metasurfaces to focus electromagnetic waves in reflection geometry," *Opt. Lett.* **37**, 4940-4942 (2012).
- [29] D. M. Lin, P. Y. Fan, E. Hasman, and M. L. Brongersma, "Dielectric gradient metasurface optical elements," *Science* **345**, 298-302 (2014).
- [30] M. Khorasaninejad, W. T. Chen, R. C. Devlin, J. Oh, A. Y. Zhu, and F. Capasso, "Metalenses at visible wavelengths: Diffraction-limited focusing and subwavelength resolution imaging," *Science* **352**, 1190-1194 (2016).
- [31] H.-T. Chen, "Interference theory of metamaterial perfect absorbers," *Opt. Express* **20**, 7165-7172 (2012).
- [32] H. R. Anderson, Fixed Broadband Wireless System Design (Wiley, 2003).

Figures:

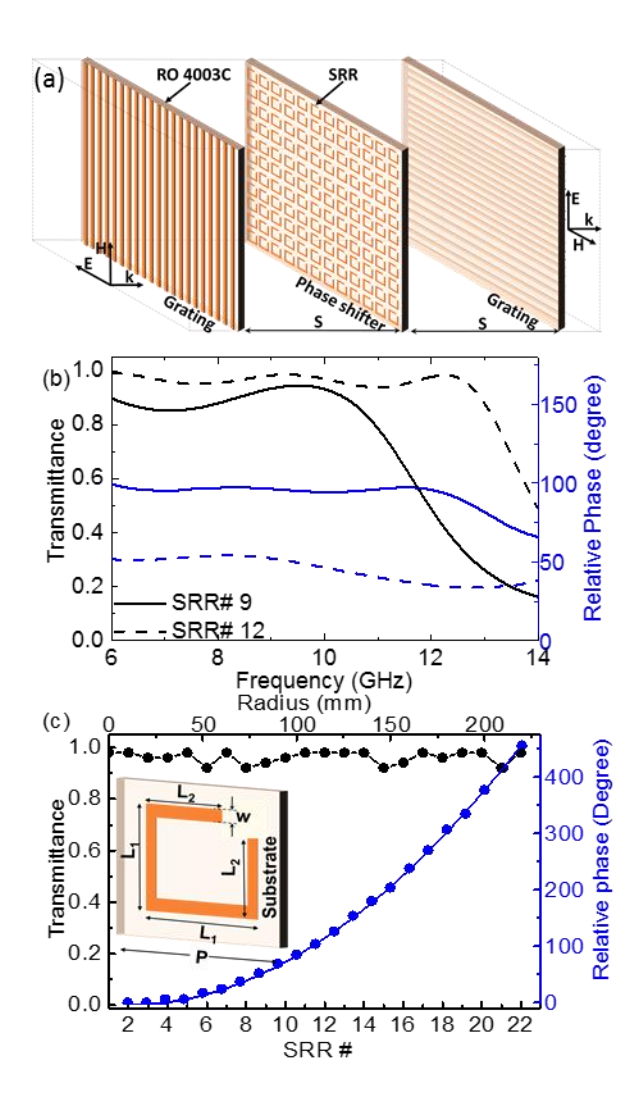


Fig. 1 (a). Schematic representation (not drawn to scale) of the metasurface lens antenna consisting of three thin layers of subwavelength metallic structures on printed circuit broads. (b) Simulated transmittance (black) and phase (blue) spectra of two SRR elements. The solid (dashed) curves represent the spectra of SRRs in zone #9 (#12) from the center. (c) Calculated and simulated phase distributions from center to edge of the lens at 9 GHz are shown as a blue solid curve and blue solid dots, respectively. The black curve shows the simulated transmittance through various SRRs. Inset: the schematic of an SRR unit cell, where P = 10 mm is the period and w = 1 mm is the width of the copper lines.

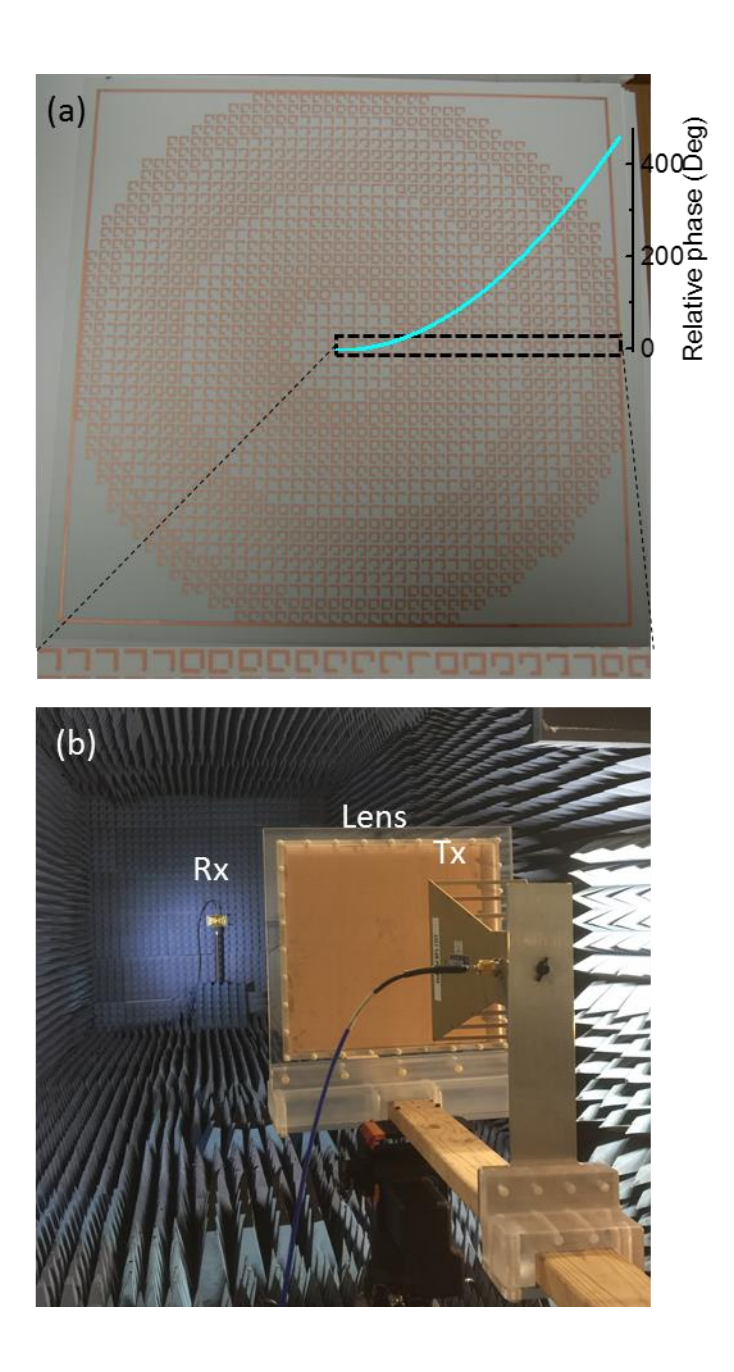


Fig. 2. (a) Photograph of the fabricated center metasurface layer containing an array of spatially variant SRRs on a 0.508 mm thick RO 4003C substrate. The cyan curve shows the required phase distribution along the lens radius according to equation (1). The bottom inset shows an expanded view of the radially distributed SRR elements and their relative orientations within the black dashed box area. (b) The experimental setup for characterizing the metasurface lens, consisting of a feed horn (Tx) and a receiving horn (Rx) inside a low noise anechoic chamber.

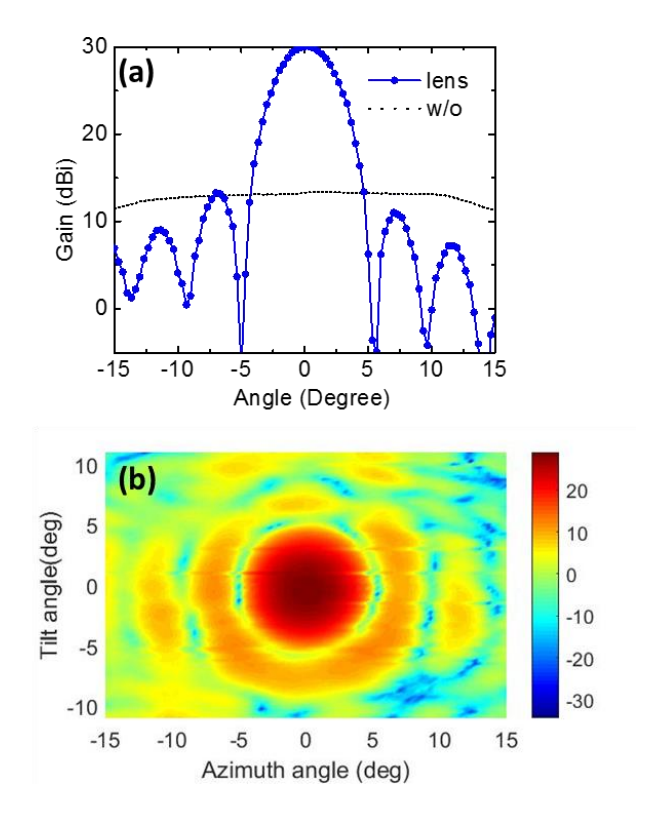


Fig. 3. (a) Measured gain for microwave radiation from a rectangular horn with (blue curve) and without (black dotted curve) the metasurface lens as a function of the azimuth (horizontal) scan angle. (b) 2D plot of power density profile from the metasurface lens antenna.

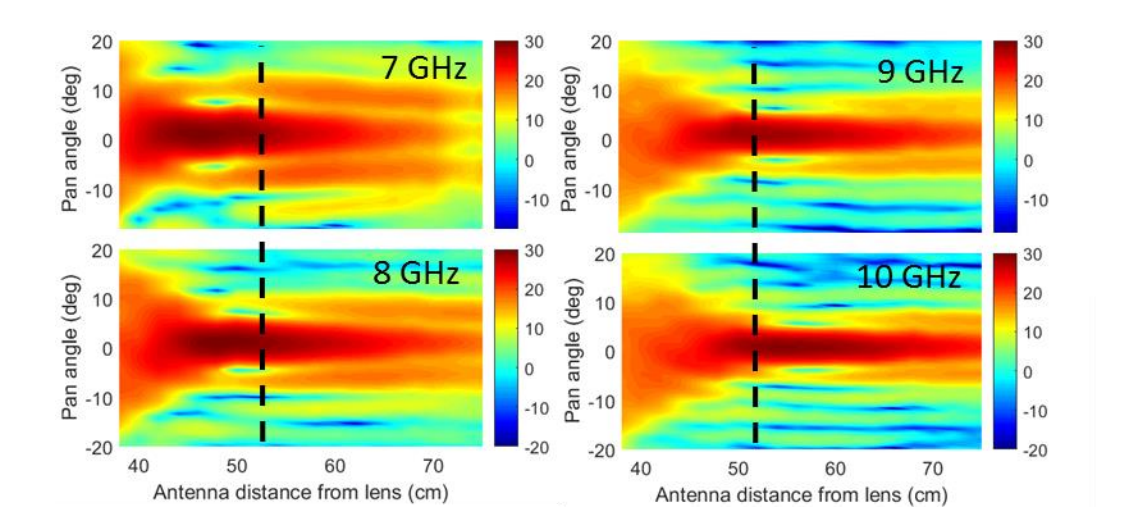


Fig. 4. Measured microwave power transmitting through the horn-fed metasurface lens antenna at different frequencies as a function of pan angle and distance (d_1) between feed horn (Tx) and lens.